

Constraints on the absorption-dominated model for the X-ray spectrum of MCG–6-30-15

C. S. Reynolds,^{1★} A. C. Fabian,² L. W. Brenneman,³ G. Miniutti,⁴ P. Uttley⁵
and L. C. Gallo⁶

¹*Department of Astronomy and the Maryland Astronomy Center for Theory and Computation, University of Maryland, College Park, MD 20742, USA*

²*Institute of Astronomy, Madingley Road, Cambridge CB3 0HA*

³*NASA/Goddard Space Flight Center, Greenbelt, MD 20771, USA*

⁴*LAEX, Centro de Astrobiología (CSIC-INTA); LAEFF, PO Box 78, E-28691, Villanueva de la Cañada, Madrid, Spain*

⁵*School of Physics and Astronomy, University of Southampton, Southampton SO17 1BJ*

⁶*Department of Astronomy and Physics, Saint Mary's University, 923 Robie Street, Halifax, NS, B3H 3C3, Canada*

Accepted 2009 April 18. Received 2009 March 18; in original form 2008 October 1

ABSTRACT

Complexities in the X-ray spectrum of the nearby Seyfert 1.2 galaxy MCG–6-30-15 are commonly interpreted in terms of a broad iron line and the associated Compton reflection hump from the innermost relativistic regions of an accretion disc around a rapidly spinning black hole. However, an alternative model has recently been proposed in which these spectral features are caused entirely by complex (ionized and partial-covering) absorption. By considering the fluorescent emission that must accompany photoelectric absorption, we show that the absorption-dominated model overpredicts the 6.4 keV iron line flux unless the marginally Compton-thick absorber responsible for the hard X-ray hump satisfies very restrictive geometric constraints. In the absence of a specific model that both obeys these geometrical constraints and is physically plausible, the relativistic-reflection model is favoured.

Key words: accretion, accretion discs – black hole physics – galaxies: individual: MCG–6-30-15.

1 INTRODUCTION

The X-ray spectrum of the nearby Seyfert 1.2 galaxy MCG–6-30-15 displays the archetypal relativistic broad iron line (Tanaka et al. 1995). The line shape is well explained by relativistic blurring (Fabian et al. 1989) of the X-ray reflection spectrum expected from the inner accretion disc around the central black hole. The redwing of the line is so broad that extreme redshifts are required indicating that the inner radius of the disc is close to the black hole and thus that the hole is rapidly spinning (Dabrowski et al. 1997; Brenneman & Reynolds 2006). In this case, much of the emission originates from the region where gravity is so strong that light bending is a large effect. This in turn can explain the apparently disconnected spectral behaviour of the source (Miniutti et al. 2003; Miniutti & Fabian 2004), with the relativistic-reflection component showing much less variation compared with the power-law continuum (Shih, Iwasawa & Fabian 2002; Fabian & Vaughan 2003; Matsumoto et al. 2003; Larsson et al. 2007). A key prediction of the disc reflection model is the presence of a powerful Compton reflection hump at ~ 20 keV which varies in step with the broad iron line; this is indeed seen in the *Suzaku* data for this object (Miniutti et al. 2007).

Miller, Turner & Reeves (2008, hereafter MTR) propose an alternative explanation in which the X-ray spectrum of MCG–6-30-15 is sculpted by multiple absorbers. A moderately photoionized absorber partially covers the primary power-law continuum source producing a 3–7 keV hump in the spectrum which mimics the redwing of a broadened iron line. The weak narrow iron line present in the spectrum is described by reflection from distant material, but that reflection spectrum must then itself be absorbed by a second photoionized and marginally Compton-thick structure in order to correctly model the powerful 20 keV hump seen in the *Suzaku* spectrum. The MTR model requires no relativistic effects and has most zones at $100r_g$ (where the gravitational radius is defined by $r_g = GM/c^2$) or further from the black hole. We note that MTR add 3 per cent systematic error to all data before comparing the various models.

In this Letter, we address the viability of the absorption-dominated model by discussing a key constraint that is not fully explored by MTR, i.e. the unavoidable connection between the hard X-ray hump and fluorescent iron line production. In both the relativistic-reflection and the absorption-dominated models, the low-energy side of the ~ 20 keV hump is shaped by the photoelectric absorption of iron. Consequently, iron fluorescence must accompany the 20 keV hump; this is true even if there is no optically thick reflection occurring at all. We argue that the only way

★E-mail: chris@astro.umd.edu

to make the presence of the hard X-ray hump compatible with the extremely weak narrow iron line is to either strongly blur much of the iron line (as in the relativistic-reflection model) or postulate a very special geometry for the system.

We present our arguments within the context of a re-analysis of the 2006 January *Suzaku* observation of MCG–6–30–15. Section 2 describes our reduction of these data. In Section 3, we examine the constraints imposed by relating the 20 keV hump to the production of iron line photons. The meaning of these spectral constraints on the geometry of the source is discussed in Section 4, and we draw our conclusions in Section 5. All error ranges are quoted at the 90 per cent confidence level for one interesting parameter ($\Delta\chi^2 = 2.71$).

2 THE SUZAKU DATA

To illustrate the iron line constraints discussed in this Letter in concrete terms, we re-analyse the combined data of the three *Suzaku* observations of MCG–6–30–15 taken on 2006 January 9–14 (150 ks), 2006 January 23–26 (99 ks) and 2006 January 27–30 (97 ks). These data have been previously presented by Miniutti et al. (2007). MCG–6–30–15 was placed at the nominal X-ray Imaging Spectrometer (XIS) aimpoint, and all four X-ray Imaging Spectrometers (XIS0–3) were operational and collecting data. However, following Miniutti et al. (2007) we only consider data from XIS2 and XIS3 which appear to show the fewest calibration artefacts. We also utilize data from the hard X-ray detector (HXD) PIN.

Reduction started from the cleaned Version-2 data products, and data were further reduced using `FTOOLS` version 6.4 according to the standard procedure outlined in the ‘Suzaku Data Reduction (ABC) Guide’. The standard filtering resulted in 338 ks of ‘good’ data from each XIS. Spectra were extracted from XIS2 and XIS3 using a circular region of radius 4.3 arcmin centred on MCG–6–30–15. Background spectra were obtained from circular source-free regions (avoiding the calibration sources) around the chip edges. Response matrices and effective area curves were generated using the `XISRMFGEN` and `XISSIMARFGEN` tools (called via the `XISRESP` script provided to us by Keith Arnaud). We use 100 000 photons per energy bin during the construction of the effective area files. We also utilize HXD/PIN data in this Letter. Standard filtering resulted in 274.2 ks of ‘good’ *Suzaku*–HXD/PIN data from which a spectrum was constructed. A PIN background spectrum was produced that models non-cosmic background. The cosmic X-ray background was included as an additional component to the spectral model as described in the *Suzaku* Data Reduction Guide. Overall, our reduction repeats that of Miniutti et al. (2007) except for the use of updated instrumental response matrices and (importantly) HXD/PIN background models.

To avoid complexities associated with the uncontroversial warm absorption components (which possess significant opacity only below 2 keV), we restrict all spectral modelling discussed here to energies greater than 2.5 keV. Thus, we examine the 2.5–10 keV XIS2/XIS3 spectra jointly with the 14–60 keV HXD/PIN spectrum.

3 CONNECTING THE IRON LINE AND THE 20 KEV BUMP

Fig. 1 (top panels) shows a fit of the relativistic-reflection model to these *Suzaku* data. In detail, the model consists of a power-law continuum together with an ionized disc reflection spectrum which has been blurred under the assumption that it originates from the inner regions of an accretion disc around a near-maximally rotating black hole. We employ the ionized reflection models of Ross & Fabian

(2005) and the relativistic smearing kernel of Laor (1991). Note that Ballantyne, Ross & Fabian (2001) have demonstrated that diluted constant-density ionized disc reflection models such as those presented by Ross & Fabian (2005) are a very good approximation to the reflection expected from the surface layers of an accretion disc in vertical hydrostatic equilibrium. Following Brenneman & Reynolds (2006) and Miniutti et al. (2007), we also explicitly model statistically significant but weak narrow emission/absorption features using narrow Gaussians centred at 6.4 keV (cold Fe fluorescent emission), 6.67 keV (He-like Fe absorption) and 6.97 keV (H-like Fe absorption). The Ross & Fabian (2005) reflection models do not include the $K\beta$ line of cold iron at 7.1 keV; our spectral model explicitly includes an additional 7.1 keV line which is smeared together with the ionized reflection model, and we see evidence for such a line in the data. The best-fitting model is comparable to that derived by Miniutti et al. (2007); the photon index of the primary power law is $\Gamma = 2.09_{-0.08}^{+0.04}$, the reflector has iron abundance $Z = 1.8_{-0.2}^{+0.3} Z_{\odot}$ and ionization parameter $\xi < 35 \text{ erg s}^{-1} \text{ cm}$, and the relativistic smearing implies an inclination of $i = 31^{\circ} \pm 1^{\circ}$, an inner disc radius of $r = 1.7 \pm 0.1 r_g$ and emissivity profile which breaks from $\beta = 5.7 \pm 0.7$ to $2.74_{-0.10}^{+0.15}$ at $r_{\text{br}} = 3.8_{-0.5}^{+0.6} r_g$.

Of greatest importance to our current argument is the fact that a powerful iron emission line accompanies the strong reflection hump. As demonstrated in Fig. 1 (top panels), the presence of such a strong line is compatible with the data only because it is strongly smeared by the relativistic effects. We demonstrate this more explicitly by fitting the X-ray hump with a reflection model that does not include any relativistic effects, as shown in Fig. 1 (middle panels). More precisely, starting with our relativistic-reflection model, we force an inner disc radius of $r_{\text{in}} = 200 r_g$ and refit the spectrum ignoring the range of energies applicable to the broad iron line (3.5–8 keV). As well as leaving a broad residual in the 3–7 keV band (corresponding to the broad iron line in the relativistic-reflection model), this model vastly overpredicts the narrow iron line.

Primarily motivated by this line-overproduction problem, MTR advocate a model in which the hard X-ray hump is mainly shaped by direct absorption rather than reflection. However, as we shall now show, an absorption-dominated model is still subject to constraints based on iron line production.

To underscore our argument, we take an extreme form of the MTR model that should be optimized to produce the least iron line emission; we assume the complete absence of X-ray reflection and suppose that the hard X-ray hump is shaped entirely by photoelectric absorption of the primary X-ray emission by a cold, high column density absorber. Of course, the fact that we see plenty of emission at low energies shows that a significant fraction of the emission must either scatter around this absorber or leak through holes in this absorber, i.e. this is a partial-covering absorber. Again, we fit this model to the *Suzaku* data ignoring the 3.5–8 keV band. This fit implies a column density of $N_{\text{H}} = (2.0_{-0.29}^{+0.36}) \times 10^{24} \text{ cm}^{-2}$ and a covering fraction of $f = 0.35 \pm 0.03$. Taking this best-fitting model and setting $f = 0$, we determine that the partial-covering absorber is removing $7.3 \times 10^{-4} \text{ photon s}^{-1} \text{ cm}^{-2}$ from the spectrum in the 7.08–20 keV (rest-frame) band; essentially all of these photons are removed by iron K-shell photoelectric absorption (which has a threshold energy of 7.08 keV). Assuming for now that the absorber covers fraction $f = 0.35$ of the sky isotropically as seen by the X-ray source, the resulting iron line emission is simply given by the product of the photoelectric absorption rate and the fluorescent yield; using the fluorescent yield appropriate for cold iron (0.347), we estimate an iron line photon flux of $2.54 \times 10^{-4} \text{ photon s}^{-1} \text{ cm}^{-2}$. For illustration, Fig. 1 (bottom panels) shows this partial-covering

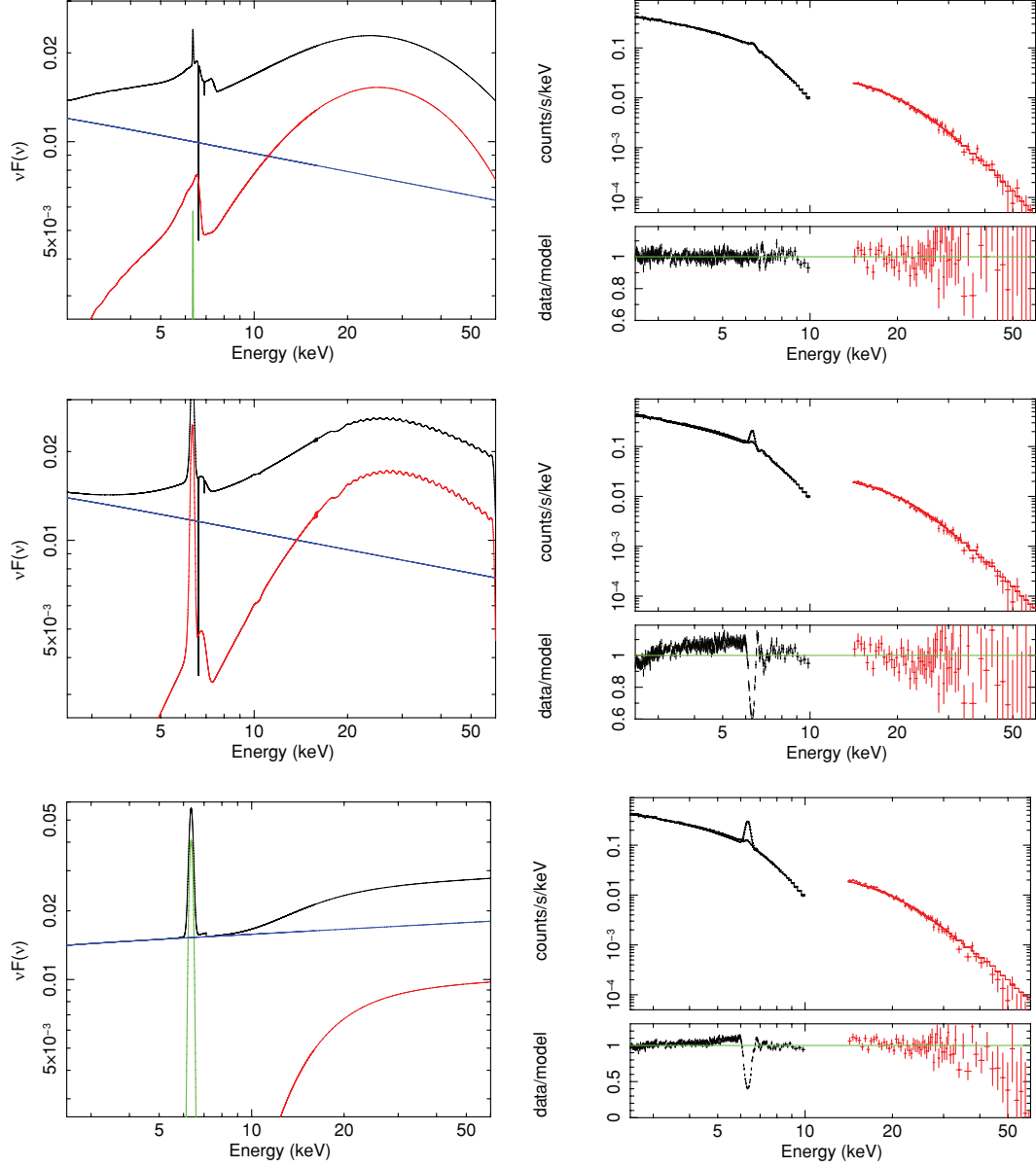


Figure 1. Top panels: relativistic-reflection model (left-hand panel) together with a fit of this model to the 2.5–60 keV *Suzaku* data. Middle panels: reflection model in which the inner disc has been fixed at $r_{\text{in}} = 200r_{\text{g}}$ (left-hand panel) together with a fit of this model to the 2.5–60 keV *Suzaku* data. Bottom panels: absorption-dominated model including the narrow iron line predicted to accompany the photoelectric absorption (left-hand panel) together with a fit of this model to the 2.5–60 keV *Suzaku* data (see Section 3 of the text for detailed descriptions of these models and the fits).

model including a 6.4 keV iron line of this strength and a width of $\sigma = 0.1$ keV.

The allowed covering fraction of this marginally Compton-thick absorber can be deduced by comparing the line photon flux predicted above with the observed values/limits. If we allow the normalization of the narrow iron line to be free in the fit to the *Suzaku* data, the observed excess at 6.4 keV (which, in the relativistic-reflection model, corresponds to the blue horn of the broad iron line) has a photon flux of 2.50×10^{-5} photon $\text{s}^{-1} \text{cm}^{-2}$; this implies that the Compton-thick absorber covers only $0.1f = 0.035$ of the sky as seen by the X-ray source. This is robust to the addition or omission of a second partial-covering absorber to mimic the broad iron line. If, instead, we use the strength of the narrow 6.4 keV iron emission line seen by the *Chandra*/High Energy Transmission

Grating (HETG) (Young et al. 2005), the corresponding photon flux (1.24×10^{-5} photon $\text{s}^{-1} \text{cm}^{-2}$) requires a covering fraction of only $0.05f = 0.0175$. Of course, if there is any other source of iron fluorescence (e.g. from reflection by very Compton-thick matter), these covering fractions must be considered upper limits.

The detailed absorption-dominated model discussed by MTR is rather more sophisticated than our ‘extreme’ case in the sense that the hard X-ray bump is modelled by an ionized reflector (that does not display any relativistic effects and hence is inferred to be at large distance from the black hole) which is absorbed by a photoionized absorber with $N_{\text{H}} \sim 5 \times 10^{23} \text{cm}^{-2}$. By construction, the iron line from the absorbed reflection spectrum describes the narrow weak 6.4 keV line seen in the *Chandra*/HETG spectrum. Using the best-fitting parameters listed in MTR, we have confirmed

that the absorber removes the same number of 7.08–20 keV photons from the observed spectrum as calculated above for our extreme case, to within a 10 per cent accuracy. Since the fluorescence yield of iron increases with ionization state, the expected fluorescence (of intermediate charge states) should be even more prominent than described above, leading to even more restrictive constraints on the covering fraction of the absorber. In principle, resonant Auger destruction (e.g. Band et al. 1990; Ross et al. 1996) within both the photoionized reflector and the absorber may reduce the iron line strength somewhat, but significant reduction (more than a factor of 2) requires a fine-tuning of the ionization parameters and the velocity structure.

The constraint discussed here is also robust to uncertainties in the iron abundance of the absorber since we are essentially comparing the iron edge to the iron line. Repeating the exercise above (with our extreme model) using an absorber with an iron abundance of 3 and $0.3 Z_{\odot}$ (all other abundances cosmic) yields predicted iron line strengths that are within 10 per cent of the cosmic abundance case.

Note that the covering fraction constraints deduced here become stronger upper limits if it is assumed that the Compton-thick absorber is in the form of clumps in a wind which is itself absorbing and giving rise to fluorescent emission.

4 DISCUSSION

Despite the fact that it is not included in the commonly employed spectral models, it is an elementary fact that fluorescent emission accompanies photoelectric absorption. As we have seen, exploiting this connection provides a powerful new constraint on the absorption-dominated model for MCG–6-30-15. In particular, the marginally Compton-thick absorber responsible for the hard X-ray hump at 20 keV cannot subtend more than 2–4 per cent of the sky as seen from the X-ray source or else it will overproduce the fluorescent iron line.

Thus, the absorption-dominated model requires a puzzling geometry. The rapid fluctuations of the continuum source on time-scales as short as ~ 100 s (Reynolds 2000; Vaughan, Fabian & Nandra 2003) suggest an X-ray source with an extent of only $\sim 2r_g$ (where we are assuming a central black hole mass of $1 \times 10^7 M_{\odot}$). However, in the MTR model, all of the absorbing structures are at $100r_g$ or further. If these structures are to only partially obscure the central compact X-ray source, either the observer must be in a special location so that the line of sight to the absorber skims the edge of the absorbing structure or the absorber must be a ‘mist’ of small clouds significantly smaller than the size of the X-ray source (in which case there is a confinement problem). So, within the context of the MTR model, the most reasonable assumption is to place an additional continuum source at a larger distance, comparable to that of the absorbing structure.

But the results of this Letter provide a further constraint that the marginally Compton-thick absorber responsible for the hard X-ray hump can subtend no more than 2–4 per cent of the sky as seen by the X-ray continuum source. If the absorber is approximately cospatial with the continuum source (as would be most natural given the partial-covering constraint), it is very difficult to envisage a geometry in which this holds true. The geometric challenge is even greater if one wishes to hypothesize that a large fraction of AGN have similar absorption-dominated models (MTR; Sim et al. 2008).

By contrast, the relativistic-reflection model does not require unusual geometries or previously unrecognized structures within the central engine. The difference spectrum (i.e. the difference be-

tween the spectrum when the source is bright to when it is faint) is well described by a power law modified by only the well-studied warm absorption components required by grating spectra; neither the broad iron line nor the reflection hump shows up in the difference spectrum (Fabian et al. 2002; Miniutti et al. 2007). The absorption-dominated model can accommodate this spectral variability, but only via unexplained correlations between the covering fraction of the absorbers and the continuum luminosity. By contrast, strong gravitational light bending is a *required and inevitable* physical process within the relativistic-reflection model and naturally explains the lack of response of the reflection features to the continuum variability (Reynolds & Begelman 1997; Miniutti et al. 2003; Miniutti & Fabian 2004). Hand in hand with the variability, the gravitational light bending of continuum X-rays towards the disc explains the fact that the strength of the reflection hump is two to three times that expected from isotropic illumination of a planar disc. A prediction of the light-bending model is that the broad iron line strength *is* correlated with the continuum luminosity in low flux states; this was confirmed by *XMM-Newton* spectroscopy of the 2000 June deep minimum state (Reynolds et al. 2004).

Note that blurring a strong line produced by absorption, in say a wind, by Compton downscattering also means that the high-energy continuum is also downscattered, to an unacceptable extent (Fabian et al. 1995).

5 SUMMARY

The relativistic-reflection model makes a bold claim, i.e. we are seeing measurable and quantifiable effects from matter within a few gravitational radii of the black hole. This gives us an astrophysical tool of enormous power for probing black hole physics. Thus, it is important to carefully assess alternative models such as the absorption-dominated model of MTR.

Suzaku observations of the prototypical broad iron line AGN MCG–6-30-15 clearly reveal a strong, hard X-ray hump (in the 10–30 keV band) which must be due to either X-ray reflection or absorption by a marginally Compton-thick absorber. In either of these cases, the low-energy side of the hump is shaped by the K-shell photoelectric absorption of iron. We consider the iron fluorescence associated with the hard X-ray hump and come to the following important conclusion: *the only way to make the presence of the hard X-ray hump compatible with the extremely weak narrow iron line is to either strongly blur much of the iron line (as in the relativistic-reflection model) or postulate a very special geometry for the system.* This conclusion is robust to mild ionization of the absorber as postulated in the MTR model (since the fluorescence yield of iron and hence the predicted strength of the line increases with ionization state). Furthermore, since our argument amounts to comparing the depth of the iron K-shell edge with the iron line, it is robust to uncertainties in the iron abundance. In the absence of a specific geometry for the absorption-dominated model which satisfies the constraints discussed here, the relativistic-reflection model is favoured.

ACKNOWLEDGMENTS

CSR thanks the National Science Foundation for support under grant AST06-07428. ACF acknowledges the Royal Society for support. LWB thanks ORAU for her current support at NASA’s GSFC as a NASA Postdoctoral Fellow. GM thanks the Ministerio de Ciencia e Innovación and CSIC for support through a Ramón y Cajal contract. PU acknowledges funding from an STFC Advanced Fellowship.

REFERENCES

- Ballantyne D. R., Ross R. R., Fabian A. C., 2001, MNRAS, 327, 10
 Band D. L., Klein R. I., Castor J. I., Nash J. K., 1990, ApJ, 362, 90
 Brenneman L. W., Reynolds C. S., 2006, ApJ, 652, 1028
 Dabrowski Y., Fabian A. C., Iwasawa K., Lasenby A. N., Reynolds C. S., 1997, MNRAS, 288, L11
 Fabian A. C., Vaughan S., 2003, MNRAS, 340, L28
 Fabian A. C., Rees M. J., Stella L., White N. E., 1989, MNRAS, 238, 729
 Fabian A. C. et al., 1995, MNRAS, 277, L11
 Fabian A. C. et al., 2002, MNRAS, 335, L1
 Laor A., 1991, ApJ, 376, 90
 Larsson J., Fabian A. C., Miniutti G., Ross R. R., 2007, MNRAS, 376, 348
 Matsumoto C., Inoue H., Fabian A. C., Iwasawa K., 2003, PASJ, 55, 615
 Miller L., Turner T. J., Reeves J. N., 2008, A&A, 483, 437 (MTR)
 Miniutti G., Fabian A. C., 2004, MNRAS, 349, 1435
 Miniutti G., Fabian A. C., Goyder R., Lasenby A. N., 2003, MNRAS, 334, L22
- Miniutti G. et al., 2007, PASJ, 59S, 315
 Reynolds C. S., 2000, ApJ, 533, 811
 Reynolds C. S., Begelman M. C., 1997, ApJ, 488, 109
 Reynolds C. S., Wilms J., Begelman M. C., Staubert R., Kendziorra E., 2004, MNRAS, 349, 1153
 Ross R. R., Fabian A. C., 2005, MNRAS, 358, 211
 Ross R. R., Fabian A. C., Brandt W. N., 1996, MNRAS, 278, 1082
 Shih D., Iwasawa K., Fabian A. C., 2002, MNRAS, 333, 687
 Sim S. A., Long K. S., Miller L., Turner T. J., 2008, MNRAS, 388, 611
 Tanaka Y. et al., 1995, Nat, 375, 659
 Vaughan S., Fabian A. C., Nandra K., 2003, MNRAS, 339, 1237
 Young A. J., Lee J. C., Fabian A. C., Reynolds C. S., Canizares C. R., Gibson R. R., 2005, ApJ, 631, 733Y

This paper has been typeset from a $\text{\TeX}/\text{\LaTeX}$ file prepared by the author.